Strategies to Optimize Biosensors Based on Impedance Spectroscopy to Detect Phytic Acid Using Layer-by-Layer Films

ARTICLE *in* ANALYTICAL CHEMISTRY · MARCH 2010

Impact Factor: 5.64 · DOI: 10.1021/ac902949h · Source: PubMed

10 AUTHORS, INCLUDING:

Marli L Moraes
Universidade Federal de São Paulo
24 PUBLICATIONS **315** CITATIONS
SEE PROFILE

Ubirajara Rodrigues Filho
University of São Paulo
89 PUBLICATIONS **763** CITATIONS
SEE PROFILE

Nara Cristina de Souza
Universidade Federal de Mato Grosso (UFMT)
40 PUBLICATIONS **301** CITATIONS
SEE PROFILE

Henrique Leonel Gomes
Universidade do Algarve
106 PUBLICATIONS **1,341** CITATIONS
SEE PROFILE

Anal. Chem. **2010,** *82,* 3239–3246

Strategies to Optimize Biosensors Based on Impedance Spectroscopy to Detect Phytic Acid Using Layer-by-Layer Films

Marli L. Moraes,*,† Rafael M. Maki,‡ Fernando V. Paulovich,‡ Ubirajara P. Rodrigues Filho,§ Maria Cristina F. de Oliveira,‡ Antonio Riul, Jr.,† Nara C. de Souza,|| Marystela Ferreira,† Henrique L. Gomes,⊥ and Osvaldo N. Oliveira, Jr.⊗

Universidade Federal de São Carlos, Campus de Sorocaba, 18052-780, Sorocaba, SP, Brazil, Instituto de Ciências Matemáticas e de Computação, Universidade de São Paulo, CP 668, 13560-970, São Carlos, SP, Brazil, Instituto de Química de São Carlos, Universidade de São Paulo, CP 780, 13560-970, São Carlos, SP, Brazil, Campus Universitário do Araguaia, Grupo de Materiais Nanoestruturados, Universidade Federal de Mato Grosso, 78600-000, Barra do Garças, MT, Brazil, Universidade do Algarve, Centro de Electrónica Optoelectrónica e Telecomunicações, Campus de Gambelas, 8005-139, Faro, Portugal, and Instituto de Física de São Carlos, Universidade de São Paulo, CP 369, 13560-970, São Carlos, SP, Brazil

Impedance spectroscopy has been proven a powerful tool for reaching high sensitivity in sensor arrays made with nanostructured films in the so-called electronic tongue systems, whose distinguishing ability may be enhanced with sensing units capable of molecular recognition. In this study we show that for optimized sensors and biosensors the dielectric relaxation processes involved in impedance measurements should also be considered, in addition to an adequate choice of sensing materials. We used sensing units made from layer-by-layer (LbL) films with alternating layers of the polyeletrolytes, poly(allylamine) hydrochloride (PAH) and poly(vinyl sulfonate) (PVS), or LbL films of PAH alternated with layers of the enzyme phytase, all adsorbed on gold interdigitate electrodes. Surprisingly, the detection of phytic acid was as effective in the PVS/PAH sensing system as with the PAH/phytase system, in spite of the specific interactions of the latter. This was attributed to the dependence of the relaxation processes on nonspecific interactions such as electrostatic cross-linking and possibly on the distinct film architecture as the phytase layers were found to grow as columns on the LbL film, in contrast to the molecularly thin PAH/PVS films. Using projection techniques, we were able to detect phytic acid at the micromolar level with either of the sensing units in a data analysis procedure that allows for further optimization.

Recent developments in the field of sensors or biosensors have shown that sensing units produced with nanostructured films are capable of a high distinguishing ability for various liquids,[1−3] pollutants[4,5] and detection of trace amounts of phenothiazines,[6] in which the principle of detection is impedance spectroscopy. Some of these systems comprise sensor arrays, as the so-called electronic tongues are based on the global selectivity concept, thus mimicking the human gustatory system in which the large amount of information associated with taste is grouped into five basic tastes, namely, salt, sweet, bitter, sour, and umami. Therefore, one may expect that the sensing units do not need to interact specifically with the tasting substance and indeed this has proven to be the case. Several types of materials have been used as transducers, including synthetic semiconducting polymers[1−4] and natural polymers.[7−9] The electrical response obtained with impedance spectroscopy varied with the sensing unit, with the high sensitivity being attributed to the nanostructured nature of the films in the sensing units, which have been fabricated using either the Langmuir−Blodgett (LB)[1−4,6,7] or the layer-by-layer (LbL) methods.[5,9,10]

* To whom correspondence should be addressed.
† Universidade Federal de São Carlos.
‡ Instituto de Ciências Matemáticas e de Computação, Universidade de São Paulo.
§ Instituto de Química de São Carlos, Universidade de São Paulo.
|| Universidade Federal de Mato Grosso.
⊥ Universidade do Algarve.
⊗ Instituto de Física de São Carlos, Universidade de São Paulo.

(1) Ferreira, M.; Riul, A.; Wohnrath, K.; Fonseca, F. J.; Oliveira, O. N., Jr.; Mattoso, L. H. C. *Anal. Chem.* **2003**, *75*, 953–955.
(2) Riul, A.; de Sousa, H. C.; Malmegrim, R. R.; dos Santos, D. S., Jr.; Carvalho, A. C. P. L. F.; Fonseca, F. J.; Oliveira, O. N., Jr.; Mattoso, L. H. C. *Sens. Actuators, B: Chem.* **2004**, *98*, 77–82.
(3) Borato, C. E.; Riul, A.; Ferreira, M.; Oliveira, O. N., Jr.; Mattoso, L. H. C. *Instrum. Sci. Technol.* **2004**, *32*, 21–30.
(4) da Silva, B. A.; Antunes, P. A.; Pasquini, D.; Curvelo, A. A. S.; Aroca, R. F.; Riul, A.; Constantino, C. J. L. *J. Nanosci. Nanotechnol.* **2007**, *7*, 510–514.
(5) Zucolotto, V.; Pinto, A. P. A.; Tumolo, T.; Moraes, M. L.; Baptista, M. S.; Riul, A.; Araujo, A. P. U.; Oliveira, O. N., Jr. *Biosens. Bioelectron.* **2006**, *21*, 1320–1326.
(6) Aoki, P. H. B.; Caetano, W.; Volpati, D.; Riul, A.; Constantino, C. J. L. *J. Nanosci. Nanotechnol.* **2008**, *8*, 4341–4348.
(7) Martins, G. F.; Pereira, A. A.; Straccalano, B. A.; Antunes, P. A.; Pasquini, D.; Curvelo, A. A. S.; Ferreira, M.; Riul, A.; Constantino, C. J. L. *Sens. Actuators, B: Chem.* **2008**, *129*, 525–530.
(8) Pereira, A. A.; Martins, G. F.; Antunes, P. A.; Conrrado, R.; Pasquini, D.; Job, A. E.; Curvelo, A. A. S.; Ferreira, M.; Riul, A.; Constantino, C. J. L. *Langmuir* **2007**, *23*, 6652–6659.
(9) dos Santos, D. S.; Riul, A.; Malmegrim, R. R.; Fonseca, F. J.; Oliveira, O. N., Jr.; Mattoso, L. H. C. *Macromol. Biosci.* **2003**, *3*, 591–595.
(10) Moraes, M. L.; de Souza, N. C.; Hayasaka, C. O.; Ferreira, M.; Rodrigues Filho, U. P.; Riul, A., Jr.; Zucolotto, V.; Oliveira, O. N., Jr. *Mater. Sci. Eng., C* **2009**, *29*, 442–447.

10.1021/ac902949h
Published on Web 03/24/2010

Sensor selectivity may be obtained using materials capable of molecular recognition, e.g., enzymes or antigens in biosensors or immunosensors, respectively.[5,10−15] Electrochemical biosensors have been produced with phytase enzyme immobilized in LbL films, which could detect phytic acid with a detection limit of 0.19 mmol L^{-1}, and is sufficient to detect phytic acid in seeds of grains and vegetables.[16] Detection was performed with amperometry, and the system was optimized by depositing LbL films of phytase alternated with poly(allylamine) hydrochloride (PAH) onto an indium−tin oxide (ITO) substrate covered with Prussian Blue (PB).[17] The motivation for studying phytic acid lies on its antinutritional role for chelating metal ions and decrease the bioavailability of proteins.[18−20]

In this study, we revisit the sensing of phytic acid, now employing impedance spectroscopy with a sensor array comprising LbL films containing phytase, which should interact specifically with phytic acid, and polyelectrolytes that have no specific interactions. The goal was to combine selectivity with the high sensitivity of the impedance technique, particularly because the small-signal impedance sensors require less instrumentation and can be adapted to have low cost in addition to a rapid analysis.[21] The choice of the LbL method[22−24] was based on its suitability for preserving activity of biomolecules. A key point was to establish optimized conditions for detection and identification of the role of the molecular recognition ability of the materials in the sensing units. Surprisingly, the distinguishing ability of the phytase-containing sensing units was not better than that with polyelectrolyte LbL films, indicating that molecular recognition does not dictate the sensor performance entirely. Therefore, other parameters such as the presence of low-frequency relaxation processes near the sensitive region (electrode) are equally important. In addition, the impedance data were treated with visualization information methods,[25] better exploring the sensitivity of the whole impedance vs frequency curves, instead of measurements at fixed frequencies.

MATERIALS AND METHODS

The sensing units were obtained from 5 -bilayer layer-by-layer (LbL) films[10] deposited onto 50 pairs of gold interdigitated electrodes having 10 μm width and being 10 μm apart from each other. The films comprised alternating layers of phytase from *Aspergillus ficuum* (EC 3.1.3.8) (1.1 units/g, IP = 4.5) with poly(allylamine) hydrochloride (PAH) or poly(vinyl sulfonate) (PVS) alternated with PAH. In all cases, 5-bilayer films were adsorbed onto a 2-bilayer, PAH/PVS LbL cushion to reduce substrate effects.[26] All materials were purchased from Sigma-Aldrich (see Figure 1). In order to characterize the film growth and the surface morphology, PAH/phytase films were deposited on quartz substrates that were previously hydrophilized as described in ref 10. For comparison, a bare gold interdigitated electrode was also used as reference.

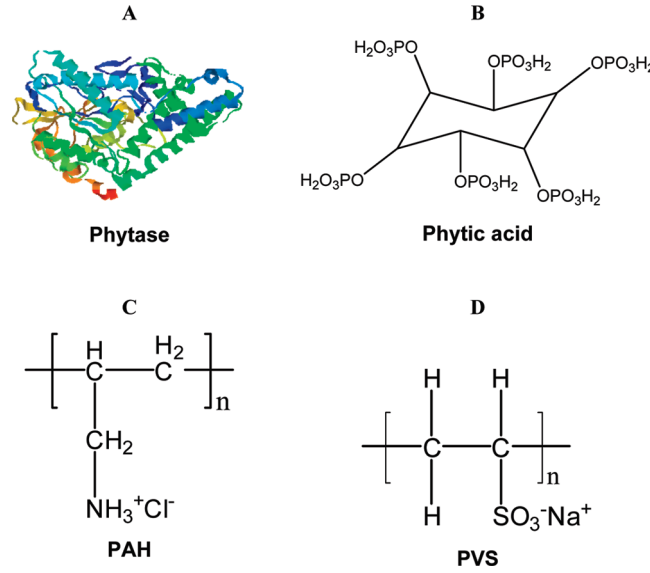

Figure 1. Structures of the materials employed: phytase (A), phytic acid (B), poly(allylamine) hydrochloride (PAH) (C), and poly(vinyl sulfonate) (PVS) (D).

The LbL films were adsorbed from a 100 mM sodium acetate buffer and solutions of PAH and PVS at 1 mg mL^{-1} and phytase at 0.2 mg mL^{-1}. All solutions had a pH of 5.5 as phytase can be used as a polyanion as its isoelectric point is 4.5,[27] and PAH is a polycation, favoring electrostatic interactions. The substrate with two bilayers of PAH/PVS was immersed in a PAH solution for 5 min, being further rinsed with sodium acetate buffer to remove loosely adsorbed molecules. Subsequently, it was immersed in the phytase solution for 10 min for enzyme adsorption, being once again washed with sodium acetate buffer. The temperature of the aqueous solution for adsorbing PAH and PVS was 25 °C. The temperature for phytase was raised to 40 °C since below that the film growth was not possible, as the optimum temperature for enzyme activity at pH 5.5 ranges from 37 to 60 °C,[28] corroborating the higher efficiency in film growth at higher temperatures according to Salomäki et al.[29]

The growth of phytase multilayers was monitored at each deposition step by measuring the absorbance at 280 nm, which

(11) Caseli, L.; Moraes, M. L.; Zucolotto, V.; Ferreira, M.; Nobre, T. M.; Zaniquelli, M. E.; Rodrigues Filho, U. P.; Oliveira, O. N., Jr. *Langmuir* **2006**, *22*, 8501–8508.
(12) Moraes, M. L.; Rodrigues, U. P.; Oliveira, O. N., Jr.; Ferreira, M. *J. Solid State Electrochem.* **2007**, *11*, 1489–1495.
(13) Campas, M.; O'Sullivan, C. *Anal. Lett.* **2003**, *36*, 2551–2569.
(14) Bae, Y. M.; Oh, B. K.; Lee, W.; Lee, W. H.; Choi, J. W. *Biosens. Bioelectron.* **2005**, *21*, 103–110.
(15) Abu-Rabeah, K.; Ashkenazi, A.; Atias, D.; Amir, L.; Marks, R. S. *Biosens. Bioelectron.* **2009**, *24*, 3461–3466.
(16) Nagashima, T.; Tange, T.; Anazawa, H. *Appl. Environ. Microbiol.* **1999**, *65*, 4682–4684.
(17) Moraes, M. L.; Oliveira, O. N.; Rodrigues-Filho, U. P.; Ferreira, M. *Sens. Actuators, B: Chem.* **2008**, *131*, 210–215.
(18) Le i, X. G.; Porres, J. M. *Biotechnol. Lett.* **2003**, *25*, 1787–1794.
(19) Raboy, V. *Trends Plant Sci.* **2001**, *6*, 458–462.
(20) Mak, W. C.; Ng, Y. M.; Chan, C. Y.; Kwong, W. K. *Biosens. Bioelectron.* **2004**, *19*, 1029–1035.
(21) Cabral, F. P. A.; Bergamo, B. B.; Dantas, C. A. R.; Riul, A., Jr.; Giacometti, J. A. *Rev. Sci. Instrum.* **2009**, *80*, 026107.
(22) Decher, G. *Science* **1997**, *277*, 1232–1237.
(23) Ariga, K.; Hill, J. P.; Ji, Q. *Phys. Chem. Chem. Phys.* **2007**, *9*, 2319–2340.
(24) Ariga, K.; Hill, J. P.; Lee, M. V.; Vinu, A.; Charvet, R.; Acharya, S. *Sci. Technol. Adv. Mater.* **2008**, *9*, 014109.
(25) Oliveira, M. C. F.; Levkowitz, H. *IEEE Trans. Vis. Comput. Graph.* **2003**, *9*, 378–394.
(26) Lobo, R. F. M.; Pereira-da-Silva, M. A.; Raposo, M.; Faria, R. M.; Oliveira, O. N., Jr. *Nanotechnology* **2003**, *14*, 101–108.
(27) Ullah, A. H. J.; Gibson, D. M. *Prep. Biochem. Biotechnol.* **1987**, *17*, 63–91.
(28) Ullah, A. H.; Sethumadhavan, K.; Lei, X. G.; Mullaney, E. J. *Biochem. Biophys. Res. Commun.* **2000**, *275*, 279–285.
(29) Salomäki, M.; Vinokurov, I. A.; Kankare, J. *Langmuir* **2005**, *21*, 11232–11240.

corresponds to the maximum in absorption, with a Hitachi U-2001 spectrophotometer. The kinetics of adsorption of a phytase layer deposited on the 2-bilayer cushion of PAH/PVS was also investigated by measuring the absorbance at distinct adsorption times. The morphology of a 10-bilayer film of PAH/phytase deposited on a quartz substrate coated with a 2-bilayer PAH/PVS cushion was studied with atomic force microscopy (AFM) using a Nanoscope IIIa (Digital Instruments) microscope with 512×512 pixels per image obtained under ambient conditions in the tapping mode. The roughness and size of the aggregates were obtained using the software provided by Digital Instruments.

For the sensing experiments, alternating current (ac) measurements were performed with a Solartron 1260A impedance/gain phase analyzer in a frequency range from 1 to 1×10^7 Hz. The experiments were conducted by soaking the electrode in a 100 mM sodium acetate pH 5.5 buffer solution (control solution) and in buffer solutions containing different concentrations of phytic acid (*myo*-inositol hexakis dihydrogen phosphate), acquired from Synth. The measurements were performed using three gold interdigitated electrodes: a bare electrode, one coated with seven PAH/PVS bilayers, and another with two PAH/PVS bilayers covered with five PAH/phytase bilayers. Each solution was measured 10 times. The data comprising the real and imaginary parts of the impedance at the various frequencies measured were processed with projection or point placement techniques.[30]

Projection techniques create visual representations aimed at providing insight into the similarity relationships among different entities or samples from a data set. They map each sample into a graphical element placed on a two-dimensional visual layout, so that similar samples are placed as close elements and dissimilar ones are placed far apart. The result is a visualization of the data samples that enables users to employ their visual perception abilities to evaluate the similarity/dissimilarity relationships among the samples or groups of samples under analysis. In this article we show that such visualizations are particularly effective to infer the behavior of different sensor assemblies.

Formally, let $X = \{x_1,x_2,...,x_n\}$ be a given set of n data samples, and let $Y = \{y_1,y_2,...,y_n\}$ be their corresponding mappings into the visual layout, with $\delta(x_i,x_j)$ being a dissimilarity function between two samples, and $d(y_i,y_j)$ a distance between the two elements mapped on the visual layout. A projection technique can be described as an injective function $f: X \rightarrow Y$ which seeks to minimize $|\delta(x_i,x_j) - d(f(x_i),f(x_j))| \; \forall \; x_i,x_j \in X$. There are many forms to implement function f (refer to ref 31 for a list of different approaches), giving rise to multiple distinct classes of projection techniques. In all of them, the desired ideal of preserving the original distances is achieved only up to a certain point, as it is normally not possible to obtain a low-dimensional representation of the original data capable of faithfully retaining all the data relationships as they exist in the original data space. The choice of the more suitable function depends on the characteristics of the data set X. In this article we employ two projection techniques, namely, Sammon's Mapping (SM)[32] and Interactive Document Map (IDMAP),[33] with which distinct levels of separation between the samples was achieved in different situations.

SM is a nonlinear technique that employs a function of the differences among the distances between the elements in the visual layout and the original computed distances between the samples, given in eq 1. It minimizes this function using an iterative nonlinear steepest descent optimization approach based on the function gradient to find a (local) minimum.

$$S_{\mathrm{SM}} = \frac{1}{\sum_{i<j} \delta(x_i,x_j)} \sum \frac{(d(y_i,y_j) - \delta(x_i,x_j))^2}{\delta(x_i,x_j)} \qquad (1)$$

The function S_{SM} may be interpreted as a measure of the amount of information loss incurred in the projection process, hence the name loss (or cost) function.

The second technique, IDMAP, performs an initial mapping of the samples to the visual layout and then improves it with a precise strategy known as Force Scheme.[34] The Force Scheme mimics a mass−spring system with attraction and repulsion forces to improve the initial placement, similar to the well-known graph-layout approaches.[35] The rationale behind this strategy is as follows: for each projected sample $y_i \in Y$, a vector $\vec{v}_{ij} = (y_j - y_i)$, $\forall \; y_i \neq y_j$ is computed, then y_i is moved in the direction of $\vec{v}_{ij}$. The amount of movement is given by

$$S_{\mathrm{IDMAP}} = \frac{\delta(x_i,x_j) - \delta_{\min}}{\delta_{\max} - \delta_{\min}} - d(y_i,y_j) \qquad (2)$$

where $\delta_{\min}$ and $\delta_{\max}$ are the minimum and maximum distances between the samples. By successful application of this process to all samples, the difference $|\delta(x_i,x_j) - d(f(x_i),f(x_j))| \; \forall \; x_i,x_j \in X$ is reduced, resulting in a more precise placement of the points, as far as distance preservation in the original space is concerned. Here $\delta(x_i,x_j)$ is taken as the Euclidean distance between the electrical impedances of samples x_i and x_j, measured in m different frequencies. Thereby, we can interpret each data sample as an m-dimensional vector embedded into an m-dimensional space.

It is worth noting the difference in the SM and IDMAP techniques, by comparing their cost functions S_{SM} and S_{IDMAP}. While IDMAP seeks to preserve as much as possible the difference $|\delta(x_i,x_j) - d(f(x_i),f(x_j))|$ for each pair of samples ($\delta_{\min}$ and $\delta_{\max}$ are only normalization factors that do not affect the distance relationships), SM actually changes the global similarity relationships, assigning more importance to smaller sample distances by dividing the (quadratic) difference $d(f(x_i),f(x_j)) - \delta(x_i,x_j))^2$ by the factor $\delta(x_i,x_j)$. Therefore, with dependence upon the distance distribution of a set of samples, one technique may be preferable to the other, e.g., if the distance values are distributed over a wide range it may be interesting to adopt SM to minimize the effect of such a large variation on the resulting projection.

(30) Paulovich, F. V.; Minghim, R. *IEEE Trans. Vis. Comput. Graph.* **2008**, *14*, 1229–1236.

(31) Paulovich, F. V.; Nonato, L. G.; Minghim, R.; Levkowitz, H. *IEEE Trans. Vis. Comput. Graph.* **2008**, *14*, 564–575.

(32) Sammon, J. W. *IEEE Trans. Comput.* **1969**, *18*, 401–409.

(33) Minghim, R.; Paulovich, F. V.; Lopes, A. A. In *Proceedings of Visualization and Data Analysis, IS&T/SPIE Symposium on Electronic Imaging*, San Jose, CA 2006; S1−S12.

(34) Tejada, E.; Minghim, R.; Nonato, L. G. *Inf. Vis.* **2003**, *2*, 218–231.

(35) Fruchterman, T. M. J.; Reingold, E. M. *Software Prac. Exper.* **1991**, *21*, 1129–1164.

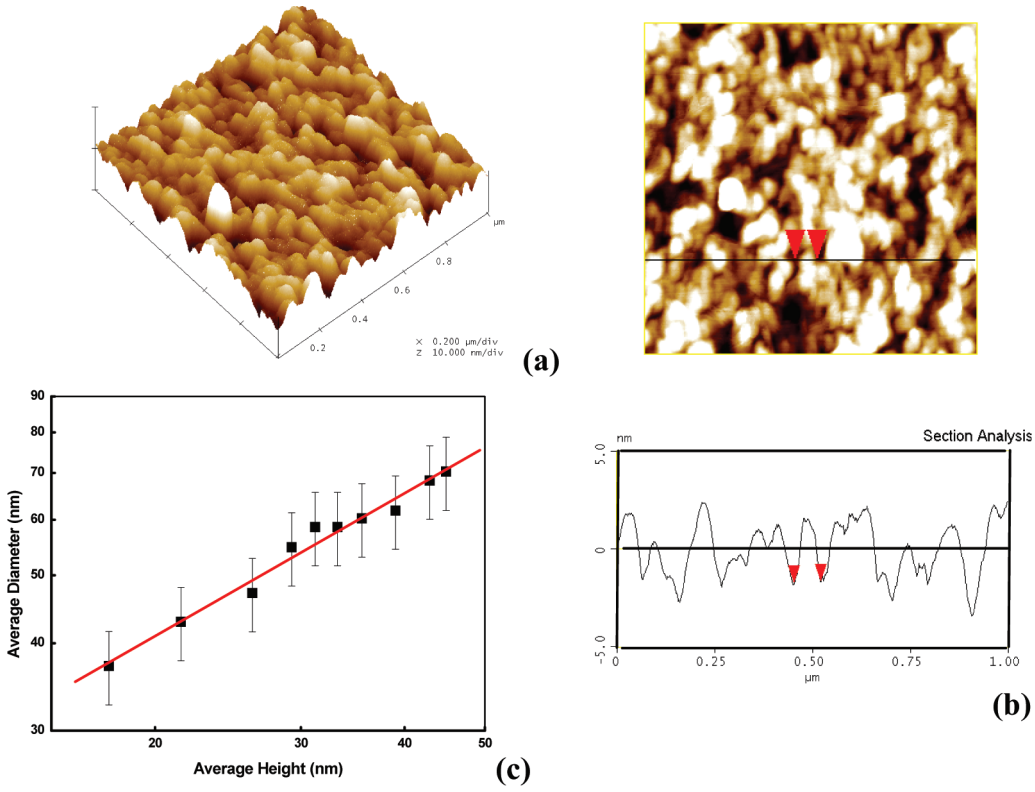

Figure 2. (a) AFM image of a 10-bilayer (PAH/phytase) LbL film adsorbed on a quartz substrate with a scanning window of 1 × 1 μm^2, (b) height profile of the film, and (c) log−log plot of the average diameter of the domains versus height for the LbL PAH/phytase films. The error bars were obtained from several scans for the same film.

A bias is introduced into the process if the measurements obtained are on different scales (depending on the frequency), leading to results that reflect mostly the difference between the larger scale measures. In order to overcome this problem, the data transformation known as standardization (STD) may be applied to the *m*-dimensional samples.[36] Given *n* sample measures, with

$$\bar{x}_j = \frac{1}{n}\sum_{i=1}^{n} x_{ij}$$

being the average value computed for the *j*th measure and

$$\sigma_j = \sqrt{\frac{1}{n}\sum_{i=1}^{n}(x_{ij} - \bar{x}_j)^2}$$

is its corresponding standard deviation. This transformation is obtained by making $x'_{ij} = (x_{ij} - \bar{x}_j)/\sigma_j$ for $1 \le i \le n$ and $1 \le j \le m$, thus mapping the values of this particular measure so that their average vanishes and their standard deviation is 1.

RESULTS AND DISCUSSION

Adsorption Mechanisms for PAH/Phytase LbL Films. The preservation of biological activity of enzymes immobilized in solid films is a major challenge for producing biosensors. The LbL method, in this context, has been proven excellent for activity preservation because one may choose a suitable template material for adsorption of the enzyme and entrained water in the film apparently helps the enzyme to retain its structure.[37] While optimizing the experimental conditions for film fabrication, we studied the film morphology and the mechanisms of adsorption with atomic force microscopy (AFM). Figure 2a shows an image for a scan window of 1 × 1 μm^2 of a 10-bilayer PAH/phytase film, whose height profile is shown in Figure 2b. From these morphological features, we may infer about the film growth.[38] For instance, upon combination of the height profile from Figure 2b and the linear increase in the average diameter for the aggregates in Figure 2c, one notes that the aggregates grow as columns.

A growth mechanism in columns is consistent with the kinetics of adsorption of a layer of phytase on an LbL film with a PAH/PVS/PAH architecture. The curve shown in Figure 3, which displays the absorption at 280 nm vs time of adsorption for the phytase layer, could be fitted with the Johnson−Mehl−Avrami (JMA) equation.[39,40] This approach allows us to get an insight on the kinetics of the film growth, despite the lack of molecular information.[38]

$$A = k_1\left[1 - \exp\left(-\frac{t}{\tau}\right)^n\right] \qquad (3)$$

(36) Tan, P.-N.; Steinbach, M.; Kumar, V. *Introduction to Data Mining*, 1st ed.; Addison-Wesley Longman Publishing Co. Inc.: Boston, MA, 2005.

(37) Caseli, L.; dos Santos, D. S., Jr.; Foschini, M.; Gonçalves, D.; Oliveira, O. N., Jr. *J. Colloid Interface Sci.* **2006**, *303*, 326–331.

(38) de Souza, N. C.; Silva, J. R.; Rodrigues, C. A.; Hernandes, A. C.; Costa, L. D.; Giacometti, J. A.; Oliveira, O. N., Jr. *Synth. Met.* **2003**, *135*, 121–122.

(39) Christian, J. W. *The Theory of Transformations in Metals and Alloys-An Advanced Textbook in Physical Metallurgy*, 2nd ed.; Pergamon Press: New York, 1981.

(40) Hay, J. N. *Br. Polym. J.* **1971**, *3*, 74–82.

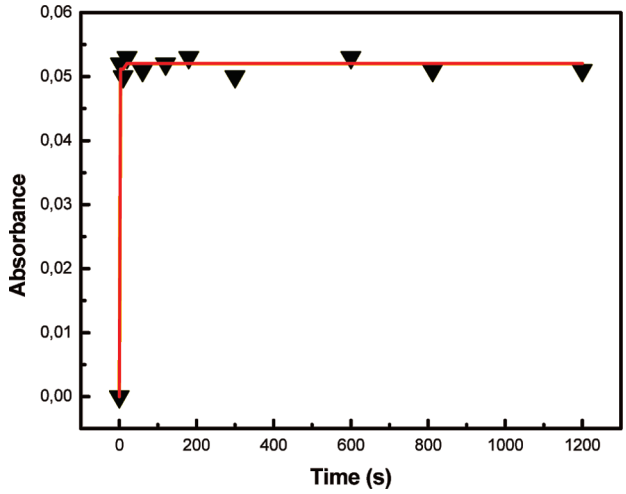

Figure 3. Film absorption (280 nm) as a function of time of adsorption for the phytase layer, where the solid line was obtained using the Johnson−Mehl−Avrami (JMA) equation.

where A is the absorbance, k and n are constants, and τ is the characteristic time for the process.[39] This phenomenological description of the adsorption kinetics using the Avrami's model has been applied successfully to the growth of polymer films.[38,40] Here the data were fitted with the parameters $k = 0.052$, $\tau = 3$ s, and $n = 1.2$. A value of $n \approx 1.2$ corresponds to a 1D adsorption, without forming new nuclei during the adsorption process with a columnar growth. Adsorption takes place with the growth of nuclei already formed in the beginning of the process, and it is a very fast process as indicated by the small characteristic time of only 3 s. The extremely fast adsorption process makes it impracticable to obtain further experimental data in the initial stages, and therefore the analysis made here with eq 3 should be taken as a rough analysis. Such fast adsorption time can indicate a monolayer or submonolayer adsorption with saturation of adsorption sites on the ITO surface, probably −OH groups. In subsidiary experiments, we obtained AFM images for a 1-layer film with phytase which display the same features of fast growth and are observed for the thicker film (results not shown). The columnar growth of the phytase layer may have important implications to the electrical properties of the sensing units made with a phytase-containing LbL film, especially because of the contrast to the other type of film used in the impedance spectroscopy studies presented here, namely, PAH/PVS LbL films that are known to be molecularly flat.

Impedance Spectroscopy with Interdigitated Electrodes Coated with LbL Films. Figures 4 and 5 display the frequency dependence of the capacitance (C) and loss (G/ω) for the electrodes coated with the PAH/PVS LbL film and phytase-containing LbL film, respectively. For the bare electrode, the capacitance and loss (results not shown) are not affected by the phytic acid concentration. The loss in the PAH/PVS is strongly suppressed by increasing the phytic acid concentration, and the relaxation frequency is shifted toward lower frequencies as the phytic acid concentration increases, as shown in Figure 4. A similar but less pronounced behavior is observed for the phytase/PAH/PVS film. The loss-frequency chart of this film displays a single sharp peak which does decrease as a function of the phytic acid concentration in the millimolar to micromolar region followed by a shift to higher frequency for the peak maximum. This is the Maxwell−Wagner relaxation process for a two-layer system, comprising in our sensors the electrolyte medium and the electrical double-layer at the coated electrode surface. Interestingly, the low frequency response of the PAH/PVS system in Figure 4b is strongly disturbed by a broad dispersion in the loss, which does not appear in the phytase-containing LbL film. This dispersion points toward the presence of a second relaxation process, which is not a well-defined peak because of the partial overlap with the Maxwell−Wagner process at 1 kHz and the dielectric leakage at low frequencies. The latter appears as a rising tail at low frequencies, visible in Figure 5b for the phytase-containing electrode. For the PAH/PVS system, these two background processes severely distort the peak, giving rise to nearly flat frequency dependence as observed in Figure 4a. At high frequencies, the capacitance decreases to become equal to the series sum of the double-layer capacitance and the bulk electrolytic capacitance. The high frequency loss is also weakly frequency dependent. Above the Maxwell−Wagner dispersion, the dissipation of energy is only related to the ac transport across the bulk electrolyte solution, being insensitive to the presence of phytic acid.

As for the capacitance results, the PAH/PVS LbL film system had a significant higher capacitance, 600 nF at 5 Hz, than the 450 nF for the phytase-containing LbL film. In addition, for the PAH/PVS system, the capacitance rose sharply at low frequencies, as expected if a second relaxation process sets in, while for the phytase-containing system the rise in capacitance was not so pronounced. The physical origin of the low frequency relaxation in the PAH/PVS coated electrode is not clear yet. A possible

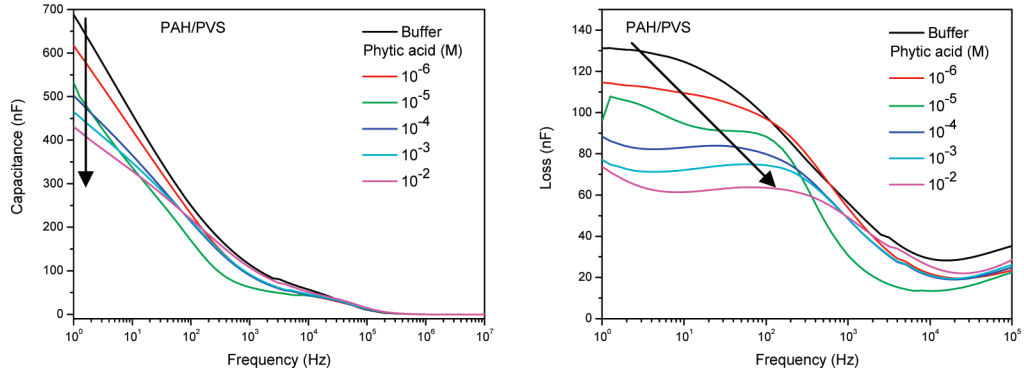

Figure 4. Capacitance (A) and loss (G/ω) (B) curves for the sensing unit made with a PAH/PVS LbL film. The curves for the 10^{-5} M concentration differ from the others, but our analysis does not allow us to determine the origin of such a difference.

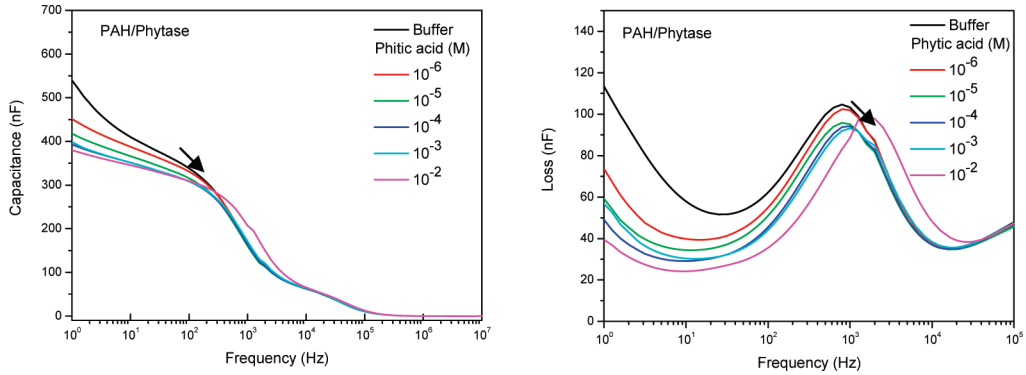

Figure 5. Capacitance (A) and loss (G/ω) (B) curves for the sensing unit made with a phytase-containing LbL film.

reason for the two relaxation processes could be the columnar growth of the films, as two types of double-layer could be established between the LbL film and solution and among the columns formed in the film.

With regard to the change in the electrical properties as the phytic acid concentration varied, one notes visually that the distinction ability of the sensing unit made with PAH/PVS LbL film could be even better than for the sensor containing phytase. From the loss curve, it is possible to infer that the limit of detection should be $\sim 4 \times 10^{-7}$ M, which could be improved by using other methods to treat the data (see below). The higher sensitivity of the PAH/PVS LbL film was unexpected because, as already mentioned, the sensitivity (and selectivity) is normally enhanced when a sensing unit contains materials capable of molecular recognition.[41] One has to consider, however, that in designing impedance-based sensors, molecular recognition is certainly important but the overall sensor performance is strongly dependent on the architecture of the LbL film on the electrode, providing a large relaxation process within the experimental observation window. The data described above illustrate clearly how these low-frequency relaxations are highly sensitive to analytes, eventually determining the sensitivity.

The decrease in the conductivity with increasing phytic acid concentration may be explained as follows. The major species of phytate at pH 5.5 is the 5-fold protonated phytate, H_5Phy^{5-}.[42] Considering the estimated diameter for phytate of ~10 Å, H_5Phy^{5-} is found to have a high charge density, i.e., it may act as kosmotrope strongly ordering the surrounding hydration layer[43,44] and establishing ionic cross-link with PAH via the protonated amine groups. The water structuring effect of kosmotropes can affect the water−polymer interaction causing conformational changes. Together with the ionic cross-linking of H_5Phy^{5-} with PAH, this water structuring may lead to a denser PAH/PVS LbL film with solvent being expelled and the ionic conductivity decreasing. Ionic cross-linking has been reported for other polyammonium salts; for instance, poly-[(1-4)-β-D-glucosamine chitosan does form salts with nitrate, iodide, fluoride, sulfate,[45,46] and trifluorsulfonate.[47] In these cross-linking polymers, no hydration water was observed, thus supporting our claim of water expelling after ionic cross-linking. Okuyama and co-workers[46] suggested that in the HI acid solution the H-bonds among the polymeric chains are broken or relaxed allowing ammonium ion protonation and entrance of iodide. Then, iodide replaces the hydration water in the crystal structure by forming H-bonds with O-6 and N-5 in the chitosan structure. Such water expelling reduces ion mobility and would result in decreased ion conductivity. In another class of poly(ammonium) electrolytes, Riley and Cook reported a decrease on hydrodynamic diameter of the poly(2-vinylpyridine) microgel by adding perchloric acid that was assigned to perchlorate ability to cross-link the polymeric chains by hydrogen bonding.[48] If perchlorate can disturb the structure of such polymeric nanogels, one should expect a higher impact from highly charged ions. Indeed, the electrostatic cross-linking capacity of highly charged ions was observed between quaternized poly(4-vinylpyridine) and hexacyanoferrate, with ensuing loss of ion mobility in these films.[49]

In the phytase-modified film, phytate is hydrolyzed yielding phosphate and inositol. In the pH at which the measurements were made, most of the phosphate groups reacted with water yielding dihydrogenphosphate. Since dihydrogenphosphate ions have a smaller charge density than phytate, its ability to alter the film architecture and hydration layer is lower. Consequently, with dihydrogenphosphate and inositol, the double-layer and the film morphology are almost unaffected, which explains the lower sensitivity of the phytase-containing sensing unit to changes in the phytic acid concentration under some experimental conditions.

Use of Information Visualization to Process the Impedance Data. The ability to distinguish among very similar samples can be enhanced considerably using statistical methods, even in cases where understanding the physicochemical mechanisms leading to the electrical response for the different films is not straightforward. Here we employed data projection techniques that are suitable for visually grouping and separating similar samples, conveying insight on sensor behavior based on the similarity relationships identified on a given set of samples.[50] Because several alternative methods exist, we explored multiple projection

(41) Zucolotto, V.; Daghastanli, K. R. P.; Hayasaka, C. O.; Riul, A., Jr.; Ciancaglini, P.; Oliveira, O. N., Jr. *Anal. Chem.* **2007**, *79*, 2163–2167.
(42) De Stefano, C.; Milea, D.; Sammartano, S. *J. Chem. Eng. Data* **2003**, *48*, 114–119.
(43) Collins, K. D. *Methods* **2004**, *34*, 300–311.
(44) Collins, K. D.; Neilson, G. W.; Enderby, J. E. *Biophys. Chem.* **2007**, *128*, 95–104.
(45) Ogawa, K.; Inukai, S. *Carbohydr. Res.* **1987**, *160*, 425–433.
(46) Lertworasirikul, A.; Yokoyama, S.; Noguchi, K.; Ogawa, K.; Okuyama, K. *Carbohydr. Res.* **2004**, *339*, 825–833.
(47) Osman, Z.; Arof, A. K. *Electrochim. Acta* **2003**, *48*, 993–999.
(48) Cook, J. P.; Riley, D. J. *Adv. Colloid Interface Sci.* **2009**, *147*, 67–73.
(49) Oh, S. M.; Faulkner, L. R. *J. Electroanal. Chem.* **1989**, *269*, 77–97.
(50) Siqueira, J. R., Jr.; Maki, R. M.; Paulovich, F. V.; Werner, C. F.; Poghossian, A.; de Oliveira, M. C. F.; Zucolotto, V.; Oliveira, O. N., Jr.; Schöning, M. J. *Anal. Chem.* **2010**, *82*, 61–65.

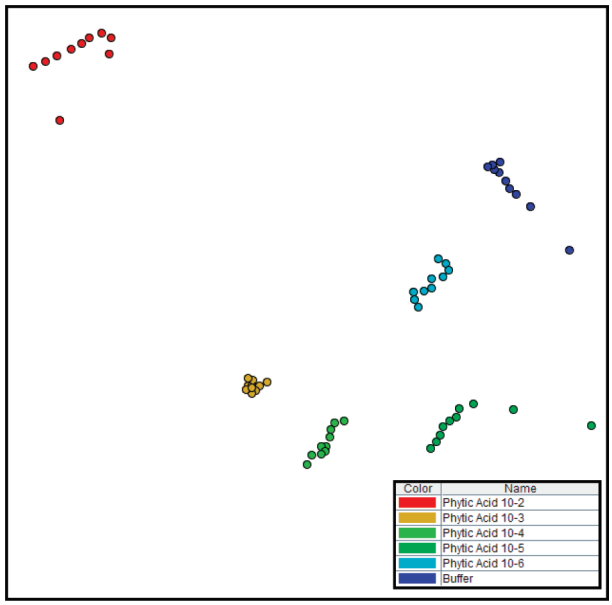

Figure 6. Visualization of the electrical impedance measures taken in the whole frequency range considered, using the sensing unit made with an LbL film of PAH/phytase. Each circle represents a complete set of measures for a particular sample, including both its real and imaginary components. The color of the circles identifies the substance. The method employed to visualize the samples was Sammon's Mapping with data standardization (SM + STD).

techniques on measurements obtained with different combinations of the sensor arrays, always considering the Euclidean distance as the sample dissimilarity measure. The optimized response was obtained with a single sensing unit made with PAH/phytase LbL film, whose data instances are shown in Figure 6, which depicts a two-dimensional projection of the data samples, represented as circles in the figure. According to the already discussed rationale of the multidimensional projections, the absolute position of the samples, i.e., their (x,y) coordinates, carries no meaning. The important information is given by the relative positioning of the samples, which is indicative of their similarity or dissimilarity: closer proximity indicates higher similarity. Notice that even if the different substances were not explicitly identified by color, the placement shows a clear separation of them in different groups. Therefore, samples with 10^{-6} M of phytic acid could easily be distinguished and if we had used lower concentrations they could probably be distinguished with the visualization methods.

As one might infer from the curves in Figure 4, the data instances could be distinguished in measurements with the PAH/PVS LbL film as well (see Figure S1 in the Supporting Information). Interestingly, for the PAH/PVS unit, good distinction among the samples was only achieved with the IDMAP technique. Therefore, the IDMAP projection works better than SM + STD for separating measurements obtained with PAH/PVS, while the converse was true for the PAH/phytase sensor. As already mentioned, these techniques adopt different cost functions to perform the data projection. IDMAP's function attempts to minimize the distance error for each sample pair, whereas the SM function actually considers the global similarity relationships by assigning more importance to smaller distances. Therefore, their different behavior is not surprising, and depending upon data characteristics, such as the presence of nonlinear relationships between data attributes and the distribution of the distances on the original data space, one technique may produce better results that the other. Because underlying distance distributions and attribute relationships in high-dimensional data sets are typically unknown, it is difficult to anticipate which technique will produce better results for a particular data set, hence, the importance of interactive exploratory tools such as the ones employed here.

The idea of using a sensor array is to exploit the so-called cross-sensitivity so that even a sensing unit that in principle is not capable of distinguishing distinct samples entirely may still contribute to enhance the overall sensitivity of the array. Indeed, this principle has been widely exploited in electronic tongues and other sensor arrays.[1−3] It may work in most cases where the data instances are selected to provide an optimized response, as it is done with impedance measurements where the frequencies are selected to yield a maximum distinguishing ability. However, when the full data set is considered, adding a new sensing unit may be deleterious as it may introduce noise. This was proven to be the case when we tried to combine two or more sensing units. Figure S2 in the Supporting Information indicates that adding the data for PAH/PVS led to a worse result than only using the data for PAH/phytase.

CONCLUSIONS

We have shown that the design of biosensors based on impedance spectroscopy should consider the dielectric relaxation processes in the sensing units, in addition to the materials suitable for reaching a high sensitivity. In biosensors employing electrochemical or optical measurements, selectivity is usually straightforward as a signal is only detected if a given reaction takes place.[51] Recently, semiselective molecules have been used to detect toxins by optical methods,[52] enlarging the number of detectable analytes. For the impedance measurements, however, changes in signal are always present for minute changes in the electrolytic solution under investigation, since the electrical properties depend on several parameters in addition to possible reactions involving the biomolecules in the biosensor. There is evidence in the literature that some selectivity could nevertheless be imparted because the specific interaction between the biomolecule and the analyte tends to yield larger changes in the electrical properties.[41] The results shown here for the phytase-containing unit and the polyelectrolyte-containing unit are in contrast to this expectation. We found that under certain experimental conditions, the relaxation processes are such that a higher sensitivity may be obtained with sensing units without molecular recognition capability. It is concluded that optimization of biosensors based on impedance spectroscopy must involve not only an adequate choice of material for the sensing unit but also the search for electrical properties whose relaxation processes are strongly affected by the analyte. The example provided here with the phytase−phytate pair may indicate that nonspecific interactions such as electrostatic cross-linking might surpass specific interactions for highly charged analytes. This may also depend on the film architecture, as the columnar growth of the phytase layer in the LbL film, inferred from the adsorption kinetics study, may

(51) Pu, K.-Y.; Liu, B. *Biosens. Bioelectron.* **2009**, *24*, 1067–1073.
(52) Taitt, C. R.; Shriver-Lake, L. C.; Ngundi, M. M.; Ligler, F. S. *Sensors* **2008**, *8*, 8361–8377.

lead to distinct electrical properties compared to the PAH/PVS LbL films that are known to be molecularly flat. Therefore, supramolecular chemistry could be exploited to maximize the response of such complex systems and improve their robustness, selectivity, and sensitivity.

While the results of an apparently poorer performance of sensing units containing biomolecules presented here may put impedance spectroscopy in a disadvantageous position in comparison to other detection principles for biosensing, it should be reminded that taking the full impedance vs frequency curve indeed allows a high sensitivity to be obtained with the phytase-containing sensing unit. This was clearly demonstrated with the use of the projection techniques, as illustrated in Figure 6. The use of visualization methods, such as the projection techniques, is in line with recent trends in analytical chemistry of resorting to more sophisticated data analysis for massive amounts of data.[53,54]

(53) Ivosev, G.; Burton, L.; Bonner, R. *Anal. Chem.* **2008**, *80*, 4933–4944.
(54) Wiklund, S.; Johansson, E.; Sjostrom, L.; Mellerowicz, E. J.; Edlund, U.; Shockcor, J. P.; Gottfries, J.; Moritz, T.; Tryg, J. *Anal. Chem.* **2008**, *80*, 115–122.

ACKNOWLEDGMENT

This work was supported by FAPESP, CNPq, and Capes (Brazil).

SUPPORTING INFORMATION AVAILABLE

Additional information as noted in text. This material is available free of charge via the Internet at http://pubs.acs.org.

Received for review December 23, 2009. Accepted March 9, 2010.

AC902949H